Trailing Edge PM Demagnetization in Surface PM Synchronous Motors: Analysis and Detection

Jigyun Jeong*, Hyeon-jun Lee*, Marcos Orviz Zapico**, Sang Bin Lee*, David Reigosa**, and Fernando Briz**

* Department of Electrical Engineering,
Korea University,
Seoul, Korea

** Department of Electrical Computer & System Engineering,
University of Oviedo,
Gijon, Spain

***Abstract*—Irreversible demagnetization of permanent magnets (PM) in PM synchronous motors (PMSM) degrades the performance and efficiency of the machine and drive system. Demagnetizing MMF applied to PMs operating at high temperature is known as one of the leading root causes of irreversible PM demagnetization. This is most likely to cause of demagnetization on the trailing edge of the PMs in all poles, as will be shown through simulation in this work. However, most of the work on detecting demagnetization faults focus on uniform or partial (local) PM demagnetization. In this paper, a comparative evaluation of back-EMF, stator current/voltage, and airgap flux analysis on the detectability of trailing edge PM demagnetization is given. It is shown that it is difficult to detect this type of fault with back-EMF or stator current/voltage based analysis, since trailing edge demagetization does not produce asymmetry between PMs. An experimental study on a 380 V, 8 pole, 1.8 kW surface PMSM with trailing edge PM demagnetization shows that airgap flux-based detection is the most reliable means of detecting this fault.**

Keywords—Airgap Flux, Back-EMF Voltage, Fault Detection, Irreversible Demagnetization, Permanent Magnet Synchronous Motors, Spectral Analysis, Stator Current.

I. Introduction

Irreversible demagnetization of PMs are known to occur due to a combination of thermal, electrical, mechanical, and/or ambient operating stresses, where high operating temperature and current are the main contributing factors [1]-[3]. Operation of the motor at excessively high temperatures typically results in uniform demagnetization of the PMs. One of the most common causes of irreversible demagnetization is the "operating point effect," which results from applying demagnetizing MMF to PMs operating at high temperature [1]–[7]. Since the magnetic axes of the demagnetizing stator MMF and PMs are not aligned during PMSM operation as shown in Fig. 1, the flux distribution of the PM is unlikely to be sinusoidal after demagnetization due to reverse MMF. Considering that the stator current vector is at or ahead of the *q*-axis during PMSM operation, the demagnetizing MMF is strongest in the trailing edge of the PM with respect to the direction of rotor rotation, as illustrated in Fig. 1. This is most likely to cause demagnetization in the trailing edge of the PM [4]. In addition, since all PMs operate at similar temperatures and the demagnetizing MMF is applied equally to all PMs, the pattern of demagnetization is likely to be similar in the PMs of all poles, unless an asymmetric fault is present in the PMSM drive system [5]-[7].

Since irreversible PM demagnetization leads to degradation in performance and reliability of the PMSM drive system, there has been active research on detecting rotor faults due to demagnetized PMs. Many off-line and on-line testing and condition monitoring approaches have been studied, where most of the methods are based on signal injection, back-emf (BEMF) voltage analysis, model-based flux estimation, and analysis of stator current/voltage or flux [3], [8]-[15]. However, most of the studies focus on detecting either 1) uniform demagnetization or 2) partial (or local) demagnetization. Detection of uniform demagnetization relies on observing the "decrease" in the magnetic strength of the PMs, and partial demagnetization is detected by observing the influence of the magnetic "asymmetry" in the motor variables.

The existing methods for detecting irreversible PM demagnetization have not been tested if they are effective for detecting demagnetization in the trailing edge, which is a common end-result of PM demagnetization. According to a thorough literature survey, the authors are not aware of any paper published on detecting trailing edge demagnetization other than [8] to the authors' best knowledge. In [8], the BEMF voltage of the non-excited phase in BLDC motors is anlayzed during operation for detecting the decrease in PM magnetic strength due to different types of demagnetization patterns including that of the trailing edge. However, the requirement of BEMF voltage measurement, a lookup table, and statistical data analysis limit its practical applicability in low cost PMSM drive sytems.

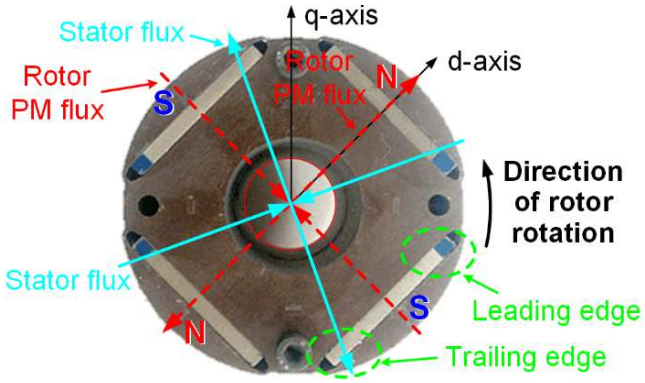

Fig. 1. Direction of PM and stator flux produced MMF during operation. Trailing edge of the rotor PM is exposed to reverse demagnetizing stator MMF.

A literature survey shows that detection of irreversible trailing edge PM demagnetization is not well understood, although there is a high probability of this fault occurring due to operating point effect. Since a reliable fault detection method for detecting this fault is required, the objective of this paper is to provide a comparative evaluation of the most common fault detection methods on the detectability of trailing edge demagnetization in surface PMSMs (SPMSM). In this work, finite element (FE) analysis is performed under excessive PM temperature and stator current to show the trailing edge demagnetization patterns caused by operating point effect. Analysis of the detectability of trailing edge demagnetization based on the BEMF voltage, stator current/voltage, and airgap flux are given to show the options for detecting this fault with high reliability. The claims are verified wih experimental testing under emulated fault conditions in surface PMSMs.

II. Operating Point Effect and Trailing Edge Demagnetization Patterns

A. Irreversible Trailing Edge Demagnetization due to Operating Point Effect

The operating point of the PM is determined at the intersection of the PM demagnetization characteristics curve and the load (permeance) curve shown in Fig. 2. NdFeB PMs have negative temperature coefficients for remanence, B_r, and coercivity, H_c, where they decrease with increase in PM temperature. For such PMs, the demagnetization curve moves as shown in Fig. 2 with increase in the temperature from T_1 to T_2, where the "knee point" of the curve is in the 2nd quadrant of the B-H curve. The load curve shifts to the left with increase in the stator current producing demagnetizing MMF. The operating point is usually restricted to the linear region of the demagnetization curve when the motor is operated within the temperature and current limits (e.g. points *a* and *b*). However, if the load curve shifts due to strong demagnetizing MMF when the PM temperature is high, the operating point can "fall off" the knee of the demagnetization curve (e.g. point *c*). Once the operating point falls off the curve at temperature T_2, the operating point is formed at the recoil line that connects point *c* and B'_{rd} with a slope identical to the original curve resulting in lower remanence at B'_{rd}. The recoil line becomes the line connecting point *b'* and B'_r even after the temperature decreases back to T_1, and the operating point does not recover to the original linear region of the B-H curve (*b-a-*B_r). The combined effect of high PM temperature and reverse MMF, is therefore, likely to decrease the remanance of the B-H curve leading to irreversible demagnetization [1]-[2]. High PM temperatures and demagnetizing MMF can be caused due a number of operating conditions such as excessive load, locked rotor, abnormal cooling, high ambient temperature, faults in the inverter or machine, or increase in core losses at high speed, etc [5]-[7].

When demagnetization occurs due to operating point effect during motor operation, the resulting pattern of the PM field after demagnetization is dependent on the relative angle between the original PM field and demagnetizing MMF. When a SPMSM is operating in the constant torque region, the stator MMF is produced only by the *q*-axis current. This applies demagnetizing MMF only on the trailing half of the PMs with respect to the direction of rotation, as can be seen in Fig. 1. The stator MMF is in the same direction as the PM field in the leading half of the PMs. When the PMSM is operating in the field weakening region with negative *d*-axis and positive *q*-axis current, the strongest demagnetizing MMF is near the trailing edge of the PM, as shown in Fig. 1. Therefore, when high stator current is applied when the PM is operating at high temperature, the trailing edges are most likely to be demagnetized. Since PMs are demagnetized with reverse MMF applied for a short period of time [5]-[7], irreversible demagnetization can occur under the conditions listed in section II.A. In addition, considering that the PM temperature distribution and stator MMF is uniform across the PMs of all poles, "symmetrical" demagnetization is likely to occur in all poles of the SPMSM.

B. Finite Element (FE) Simulation

A finite element (FE) simulation was performed on an 8 pole surface PMSM used for the experimental study in section IV. The surface PMSM has 12 slots and concentrated stator winding, as shown in the FE model in Fig. 3. This model is used for simulating the in-service demagnetization pattern in this section and also for simulating the detectability of trailing edge demagnetization in section III. The demagnetization pattern with the temperature of the N35SH PM set at 180°C, and a reverse demagnetizing MMF applied by setting the

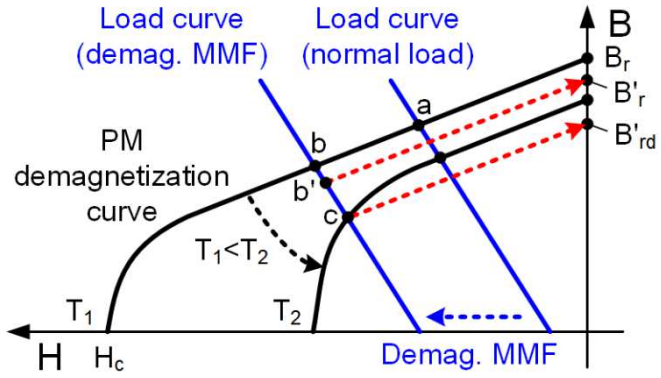

Fig. 2. PM demagnetization and load (permeance) curves for describing PM demagnetization due to "operating point effect" under high temperature and reverse demagnetizing MMF.

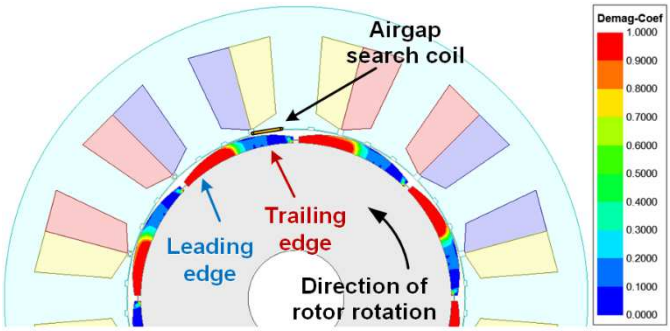

Fig. 3. Finite element simulation model of 8 pole surface PMSM

current to 5 times the rated stator current for 5 msec, is shown in Fig. 3. The flux distribution of the PMs show that demagnetization occurs in the trailing edges of the PMs in all poles, which is consistent with the predictions made. Additional results with the PM temperature set at 120°C, 150°C, and 180°C, and current set to x1, x2.5, x5, x7.5 of the rated current for 5 msec are summarized in Fig. 4. The flux density distribution with the PMSM exposed to the temperature and demagnetizing MMF (current) conditions are summarized for cases of the current vector aligned to the *q*-axis (constant torque region) and 30° ahead of the *q*-axis (field weakening region) in Figs. 4(a)-(b), respectively. The results in Fig. 4(b) show that the leading edge is also likely to be demagnetized during field weakening operation with non-zero *d*-axis current. It is clearly shown in Fig. 4 that the likelihood of trailing edge demagnetization increases with operating temperature and demagnetizing MMF due to high stator current. The FE analysis of demagnetized PMSMs shows that trailing edge demagnetization is likely to occur during service. The results also show that demagnetization occurs symmetrically in the trailing edge of the PMs of all poles. Considering the likelihood of this fault, it is important to understand what the performance of existing test methods for detecting PMSMs demagnetized in the trailing edges.

III. Assessment of Existing Methods for Detecting Trailing Edge Demagnetization

A. FE Model for Trailing Edge and Partial Demagnetization

To demonstrate the detectability of trailing edge and partial demagnetization through an FE study, the two conditions were produced by applying reverse MMF to the PMs operating at high temperature, as described in section II.B. The *q*-axis stator current was set at 10x the rated current with all the PMs set at 120°C for trailing edge demagnetization, and only one of eight PMs set at 120°C for partial demagnetization in the Fig. 3 model. The FE simulation was performed with the motor operated at 1125 rpm (75 Hz) under full load conditions. The flux linkage through the airgap search coil spanning 30 electrical degrees (shown in Fig. 3) are plotted in Fig. 5 to show the pattern and degree of demagnetization. It can be seen that there is a decrease and distortion in all PMs with trailing edge demagnetization (red dotted line), whereas only one of the poles (2nd positive pole) is influenced with partial demagnetization (yellow dashed line). The conditions of the healthy and two types of faulty SPMSMs are used for a comparative evaluation of the detectability of existing methods.

B. Off-line Detection Methods

The most effective means of detecting any type of demagnetization is to directly measure the distribution of the PM flux on the rotor surface after removing the rotor from the stator. This allows direct measurement of the flux distribution of the individual PMs with high sensitivity. However, it is very difficult to perform this off-line test, as it requires motor disassembly, rotor removal, and a specialized test setup for constant speed rotor rotation and PM flux measurement.

The "average" magnetic strength of the PMs can be measured indirectly without motor disassembly by comparing the BEMF voltage measured under the same operating speed [9]-[10]. The decrease in PM strength can be measured with the BEMF voltage since it is propotional to the flux density of the PM. The BEMF voltage with the rotor rotated at 75 Hz under partial and trailing edge demagnetization are shown in Fig. 6 along with the BEMF voltage of a healthy rotor. The results show that the decrease in BEMF voltage can be detected with both types of demagnetization shown in Fig. 5. However, the B_r is dependent on the PM temperature where it can decrease more than 1% with 10°C increase in temperature for NdFeB PMs, and therefore, BEMF voltage measurements

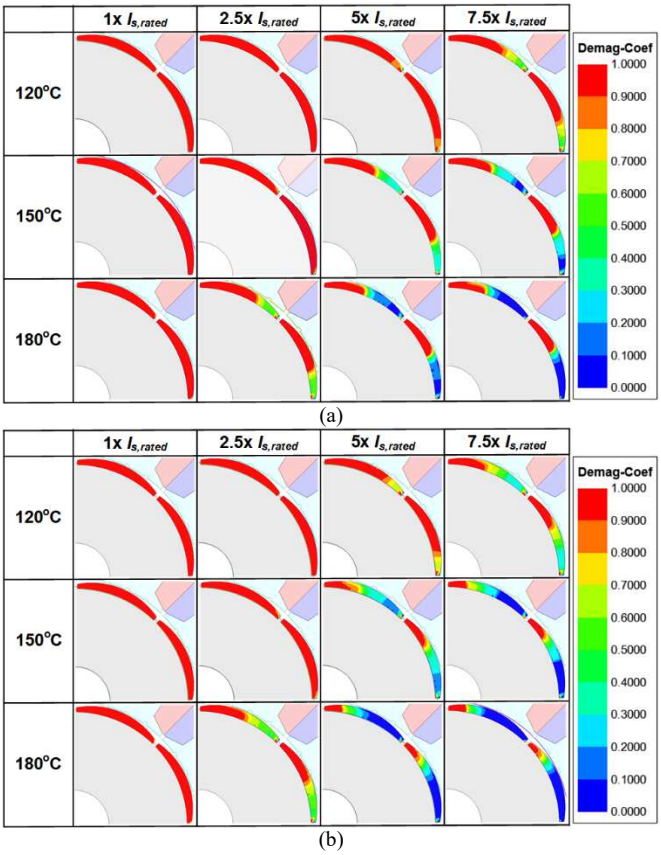

Fig. 4. FE simulation result of demagnetization after applying 1x, 2.5x, 5x, 7.5x of rated stator current in (a) *q*-axis (constant torque region) and (b) 30° ahead of *q*-axis (flux weakening region) for 5 msec.

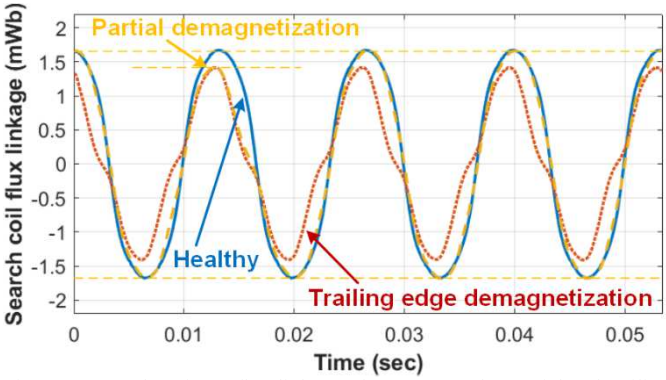

Fig. 5. FE results: airgap flux linkage of SPMSM under partial and trailing edge demagnetization.

must be taken under identical PM temperature conditions for an accurate assessment on demagnetization. The BEMF voltage is also not sensitive to the distortion in the flux distribution, since it relies on the measurement of the flux using the stator winding with a wide coil span over all the PM poles. Although there is some distortion in the harmonic content, it is not evident or predictable. Therefore, the BEMF voltage can only provide information on the "average" strength of the PMs of all the poles. In addition, the test is cumbersome, since the rotor must be rotated at constant speed. If the BEMF voltage is used for on-line detection of PM demagnetization, the stator voltage measurement is required and the PM temperature must be known.

C. On-line Detection Methods

Many on-line methods for detecting demagnetization based on PMSM models and analysis of the stator current/voltage, and airgap flux spectra have been studied to overcome the limitations of off-line testing described above [8]-[15]. Demagnetization can be detected on-line using the PM flux estimated from a mathematical model [11]. However, it has the same limitation as the BEMF voltage measurement in that it relies on monitoring of the "average" PM strength of all poles. Therefore, it is not sensitive to distortion in the flux distribution due to partial or trailing edge demagnetization unless the degree of demagnetization is severe. It is also dependent on variation in PM temperature and model parameters.

The underlying principle behind detecting demagnetization based on the spectral analysis of the BEMF voltage, stator current/voltage, or airgap flux are identical in that they rely on observing the "once per revolution (1x)" related frequency components. This component also known as the rotor rotational frequency, f_r, is expressed as

$$f_r = f_s/p, \tag{1}$$

where f_s is the fundamental frequency, and p is the number of pole pairs. Faults in the rotor of PMSMs give rise to integer multiples of f_r sidebands with respect to f_s given by

$$f_{fault} = f_s \pm k \cdot f_r = (1 \pm \frac{k}{p}) \cdot f_s, \tag{2}$$

where k is an integer [11]. The f_r related components are produced by any type "asymmetry" in the rotor, and are sensitive to demagnetization that produce asymmetry between the poles such as partial demagnetization [11]-[12].

When on-line BEMF voltage or current spectrum analysis is used, the f_{fault} component given in (2) is used for detecting asymmetry due to PM demagnetization. This component is not effective for detecting demagnetization that is uniform or in one end of the PMs of all poles, since there are no f_r-related asymmetries produced. The asymmetry in the individual PMs due to trailing edge demagnetization cannot be observed in the BEMF or stator current spectra since it relies on the voltage induced in the stator winding with a wide coil span over all the PM poles. On-line BEMF or stator current spectrum analysis is not neccesarily capable of detecting asymmetry between the PMs. It was shown in [9]-[10], [13] that the detectability of partial demagnetization with BEMF voltage or current spectrum analysis depends on the PMSM pole/stator slot combination and stator winding structure. In [16]-[17], it was shown that the detectability is also influenced by the bandwidth and gain of the current controller that regulates the current to a sinewave, making it necessary to observe the voltage spectrum instead. Therefore, the detectability of partial demagnetization depends on PMSM and controller design. There was no noticeable change in the stator current or voltage spectra under trailing edge or partial demagnetization in the FE simulation of the test SPMSM shown in Fig. 3, as predicted.

The distribution of the flux in the individual PMs can be clearly observed if the airgap flux density or airgap search coil voltage is measured with a flux sensor or search coil. The FE results of the search coil voltage with the motor operated at 75 Hz at rated load is shown in Fig. 7. Although this requires installation of search coils or flux sensors inside the motor, any type of demagnetization including trailing edge demagnetization can be detected and classified with high sensitivity since flux is directly measured from the rotor surface. Airgap flux sensors are currently being actively investigated as a low cost means of rotor fault detection (eccentricity, demagnetization) [14], partial discharge detection in the stator winding insulation [18], PM temperature estimation [19], and also for enhancement of control performance [20]. The analysis of the detectability of partial and trailing edge demagnetization with existing fault detection methods shows that airgap flux montoring is the only method capable of detecting trailing edge demagnetization.

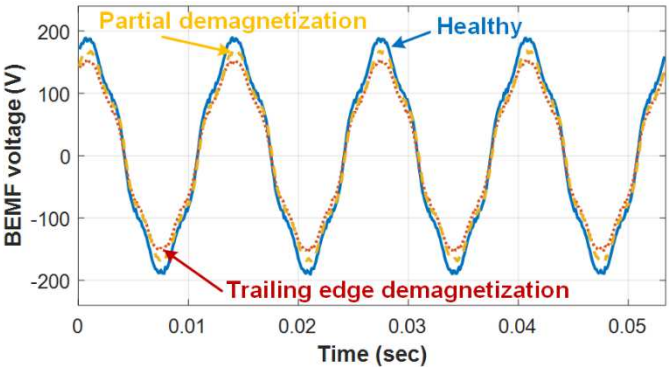

Fig. 6. FE results: BEMF voltage induced in stator winding of SPMSM under partial and trailing edge demagnetization.

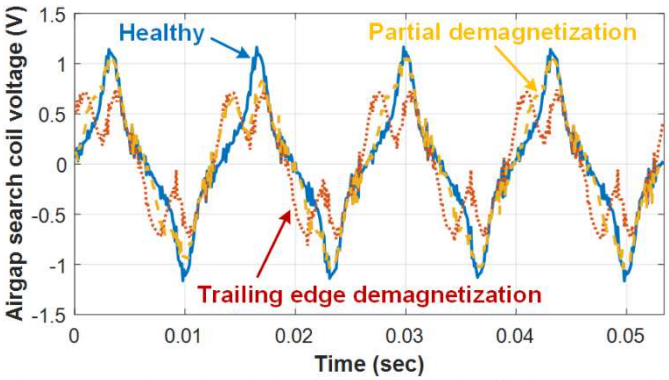

Fig. 7. FE results: voltage induced in airgap search coil of SPMSM under partial and trailing edge demagnetization.

IV. Experimental Results

A. Experimental Setup

The detectability of trailing edge demagnetization presented in section III was verified on a 1.8 kW, 8 pole, 12 slot concentrated stator winding SPMSM shown in Fig. 8. Demagnetization was produced by injecting reverse MMF to the trailing edge of the PM(s) by applying 100A DC stator current to the q-axis through a rectifier, while heating the individual PMs shown in Fig. 8(b). The temperature of all 8 PMs on the drive end were increased above 150°C with a heating gun with the rotor placed and fixed to the stator to produce trailing edge demagnetization. For producing the partially demagnetized sample, the drive end of one PM was heated above the maximum temperature when applying the reverse MMF. The flux density of the PMs were measured after demagnetization with Hall sensors placed 2 mm from the PM surface with the rotor removed from the stator, while rotating the rotor at 10 rpm. The phase to phase BEMF voltage was measured off-line, while rotating the rotor with the SPMSM load motor at 75 Hz.

To evaluate the detectability of demagnetization with different methods listed in section III, the stator voltage/current, and airgap flux were acquired at 10 kHz for the healthy and demagnetized samples. Commercial sensors were used for stator voltage/current measurements while operating the SPMSM with a commercial inverter at 75 Hz under rated load condition. A 5-turn search coil that spans 30° (electrical) was installed around 1 stator slot for measurement of airgap flux, as shown in Fig. 8(a).

B. Experimental Results

The Hall sensor measurements of the PM surface flux density are shown in Fig. 9 for the samples with partial and trailing edge demagnetization. For the trailing edge demagnetization sample, it can be seen that the trailing edges of all PMs have been demagnetized as in the case of the FE simulation in Fig. 5. There is some asymmetry between the PMs due to the uneven PM temperature distribution when the reverse MMF was applied. For the sample with partial demagnetization, the flux density of the PM in 1 pole (1st positive pole) has decreased from that of the healthy rotor. The BEMF voltage measurements with the healthy and demagnetized rotors are shown in Fig. 10. Decrease in the voltage magnitude due to the decrease in the average magnetic strength could be observed for both demagnetized rotors, as observed in the FE results in Fig. 6. The distortion in the BEMF voltage waveform was not very clear or predictable in the frequency spectrum. The main limitation of the test is that it is difficult to perform regularly, and requires the BEMF voltage to be measured under identical speed and PM temperature conditions.

The stator current waveforms and frequency spectra measured with healthy and demagnetized rotor samples with the speed controlled at 75 Hz (rated load) are shown in Fig. 11. There was no noticeable change in the stator current harmonic content or the f_r sideband components given in (2) with trailing edge demagnetization, and there was minor increase in the f_r sidebands with partial demagneization. This can be attributed to the lack of f_r-related asymmetry between PMs with trailing edge demagnetization, as in the case of the BEMF voltage. In addition, the motor structure and current controller masks the effect of harmonics for both trailing edge and partial demagnetization and suppresses the f_r-related harmonics. The f_r sideband components were not observable in the stator voltage spectrum as well for the demagnetized samples. There was an increase in the magnitude of the fundamental component of the stator current, since higher current is required for speed control with reduced PM flux.

The airgap search coil voltage waveforms are shown in Fig. 12 for the healthy and demagnetized rotor samples under 75 Hz rated load operation. The distortion in the airgap flux under trailing edge demagnetization is evident, where all the poles are demagnetized in a similar pattern. It can also be seen that there is distortion in 1 pole (2nd positive pole) with partial

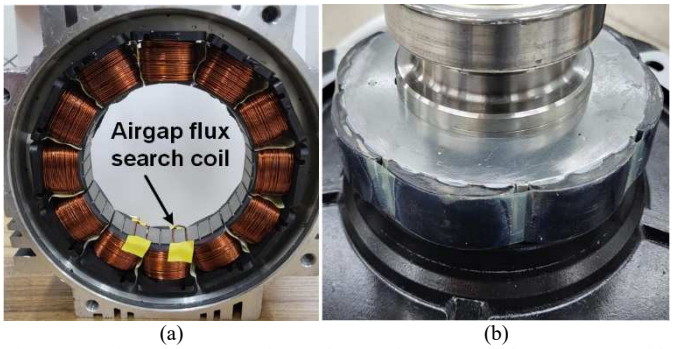

(a) (b)

Fig.8. Experiment setup: 8 pole, 1.8 kW Surface PM synchrnous motor with airgap flux search coil installed.

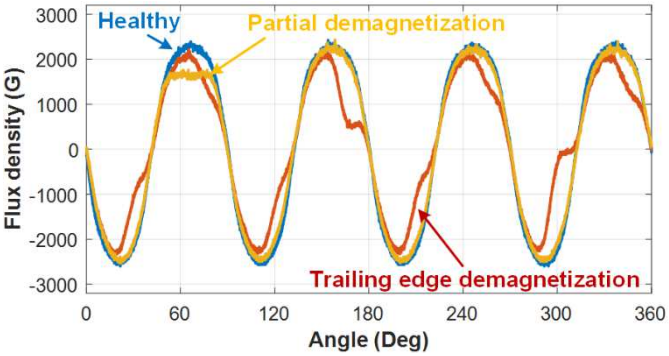

Fig.9. Experimental results: Hall sensor measurement of flux distribution on the surface PMSM rotor for healthy and demagnetized samples with rotor removed from stator.

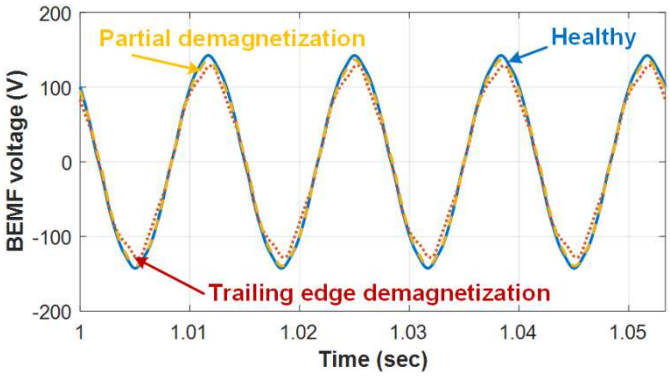

Fig.10. Experimental results: BEMF voltage measurement for healthy and demagnetized samples under rotation at 75 Hz with load motor

demagnetization. The pattern of distortion in the airgap search coil voltage for the demagentized samples in Fig. 12 is similar to the simulated waveforms in Fig. 7. The test results in Figs. 10-12 show that airgap flux analysis is the only means of dectecting trailing edge demagnetization and distinguishing it from partial demagnetization. The narrow 30º span of the airgap search coil enables reliable detection of the distortion in the flux distribution caused by any type of demagnetization, since it measures the flux directly at the PM rotor surface. Although installation of a low-cost search coil is required, it has the potential of providing many benefits including rotor faults (demagnetization and eccentricity), partial discharge detection, PM temperature estimation, and control performance enhancement.

V. Conclusion

Although demagnetization in the trailing edge of the PM due to operating point effect is a very common end result of demagnetization that occurs in PMSMs, there has not been much work done on detecting this type of fault. In this work, the detectability of trailing edge demagnetization using existing methods such as BEMF voltage measurement, and analysis of stator current/voltage, and airgap flux are evaluated through finite element analysis and experimental testing. The analysis and experimental results on a 1.8 kW SPMSM show that PMs demagnetized on the trailing edge is difficult to detect with BEMF voltage or stator current measurements presented in the literature, because the f_r related asymmetry is not produced. It is shown that airgap flux-based monitoring is the only method that can provide reliable detection of trailing edge demagnetization and distinguish it from other types of faults.

References

[1] J.R. Hendershot, T.J.E. Miller, *Design of brushless permanent magnet motors*, Motor Design Books LLC, Munich, Germany, 2010.

[2] T.J.E. Miller, *SPEED's electric motors*, University of Glasgow, 2010.

[3] J. Hong et al., "Detection and classification of rotor demagnetization and eccentricity faults for PM synchronous motors," *IEEE Trans. Ind. Appl.*, vol. 48, no. 3, pp. 923-932, May/June 2012.

[4] H. Kim, J. Hur, "Dynamic characteristic analysis of irreversible demagnetization in SPM- and IPM-type BLDC motors," *IEEE Trans. Ind. Appl.*, vol. 53, no. 2, pp. 982-990, March/April 2017.

[5] J. D. McFarland, T. M. Jahns, "Investigation of the rotor demagnetization characteristics of interior PM synchronous machines during fault conditions," *IEEE Trans. Ind. Appl.*, vol. 50, no. 4, pp. 2768-2775, July/Aug. 2014.

[6] K. Kim, Y. Lee, J. Hur, "Transient analysis of irreversible demagnetization of permanent-magnet brushless dc motor with interturn fault under the operating state," *IEEE Trans. Ind. Appl.*, vol. 50, no. 5, pp. 3357-3364, Sept./Oct. 2014.

[7] G. Choi, Y. Zhang, T. M. Jahns, "Experimental verification of rotor demagnetization in a fractional-slot concentrated-winding PMSM under drive fault conditions," *IEEE Trans. Ind. Appl.*, vol. 53, no. 4, pp. 3467-3475, July/Aug. 2017.

[8] D.-H. Kim, J. H. Im, U. Zia, J. Hur, "Online detection of irreversible demagnetization fault with non-excited phase voltage in brushless dc motor drive system," *Proc. of IEEE ECCE*, pp. 748-753, 2020.

[9] J. C. Urresty, J. R. Riba, L. Romeral, "A back-emf based method to detect magnet failures in PMSMs," *IEEE Trans. Magn.*, vol. 49, no. 1, pp. 591-598, Jan. 2013.

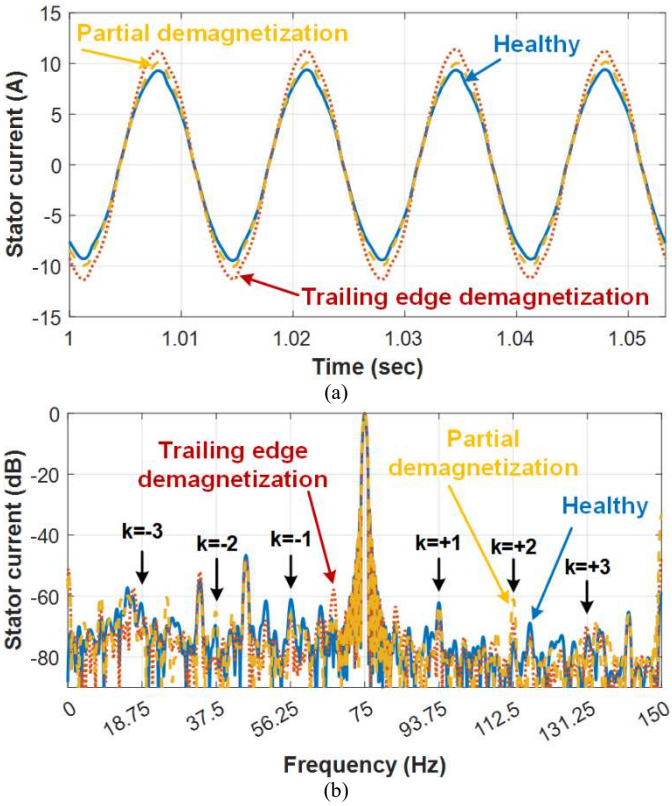

Fig.11. Experimental results: stator current (a) waveform and (b) spectrum for healthy and demagnetized samples.

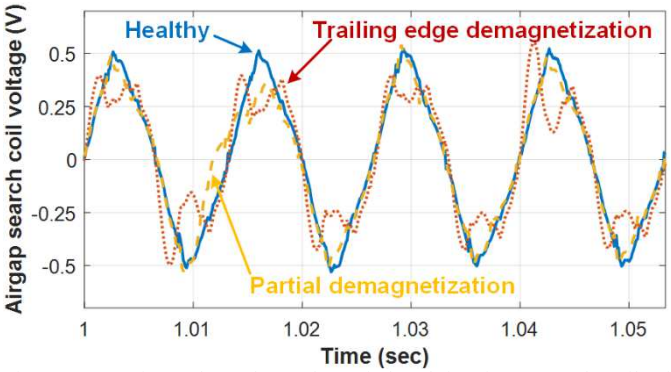

Fig.12. Experimental results: voltage induced in airgap search coil of SPMSM for healthy and demagnetized samples.

[10] M. Zafarani, T. Goktas, B. Akin, S.E. Fedigan, "An Investigation of Motor Topology Impacts on Magnet Defect Fault Signatures," *IEEE Trans. Ind. Electron.*, vol. 64, no. 1, pp. 32-42, Jan. 2017.

[11] W. le Roux, R.G. Harley, and T.G. Habetler, "Detecting rotor faults in low power permanent magnet synchronous machines," *IEEE Trans. on Power. Electr.*, vol. 22, no. 1, pp. 322-328, Jan. 2007.

[12] S. Rajagopalan, J.M. Aller, J.A. Restrepo, T.G. Habetler, R.G. Harley, "Detection of rotor faults in brushless DC motors operating under nonstationary conditions," *IEEE Trans. Ind. Appl.*, vol. 42, no. 6, pp. 1464-1477, Nov./Dec. 2006.

[13] T. Goktas, M. Zafarani, K.W. Lee, B. Akin, T. Sculley, "Comprehensive analysis of magnet defect fault monitoring through leakage flux," *IEEE Trans. Magn.*, vol. 53, no. 4, pp. 1-10, April 2017.

[14] M. S. S. Rafaq et al., "Airgap search coil based identification of PM synchronous motor defects," *IEEE Trans. Ind. Electron.*, vol. 69, no. 7, pp. 6551-6560, July 2022.

[15] Y. Park et al., "Online detection and classification of rotor and load defects in PMSMs based on hall sensor measurements," *IEEE Trans. Ind. Appl.*, vol. 55, no. 4, pp. 3803-3812, July/Aug. 2019.

[16] S. Rajagopalan, T. G. Habetler, R. G. Harley, T. Sebastian, B. Lequesne, "Current/voltage-based detection of faults in gears coupled to electric motors," *IEEE Trans. Ind. Appl.*, vol. 42, no. 6, pp. 1412–1420, Nov./Dec. 2006.

[17] W. L. Roux, R. G. Harley, T. G. Habetler, "Detecting faults in rotors of PM drives," *IEEE Ind. Appl. Mag.*, vol. 14, no. 2, pp. 23-31, Mar./Apr. 2008.

[18] H.J. Lee, et al., "Inverter-embedded partial discharge testing for reliability enhancement of stator winding insulation in low voltage machines," *Proc. of IEEE ECCE*, pp. 4724-4730, 2021.

[19] H. Lee, et al., "Airgap flux search coil-based estimation of permanent magnet temperature for thermal protection of PMSMs," *Proc. of IEEE ECCE*, pp. 1-8, Oct. 2022.

[20] Y. Kwon, S. Sul, N.A. Baloch, S. Morimoto, M. Ohto, "Design, modeling, and control of an IPMSM with an asymmetric rotor and search coils for absolute position," *IEEE Trans. Ind. Appl*., vol. 52, no. 5, pp. 3839-3850, Sept./Oct. 2016.